14. Hilton TC, Thompson RC, Williams HJ, Seiylors R, Fulmer H, Stowers SA. Technetium-99m-sestamibi myocardial perfusion imaging in the emergency room evaluation of chest pain. *J Am Coll Cardiol* 1994;23:1016–1022.
15. Cuocolo A, Soricelli A, Nicolai E, et al. Technetium-99m-tetrofosmin regional myocardial uptake at rest: relation to severity of coronary artery stenosis in previous myocardial infarction. *J Nucl Med* 1995;36:907–913.
16. Stowers SA. Myocardial perfusion scintigraphy for assessment of acute ischemic syndromes: can we seize the moment? *J Nucl Cardiol* 1995;2:274–277.
17. Matsunari I. Personal computer-based integrated image analysis system interfaced to a SPECT system. *Medical Review (Toshiba) (in Japanese)* 1994:18–2:12–16.
18. Ficaro EP, Fessler JA, Ackermann RJ, Rogers WL, Corbett JR, Schwaiger M. Simultaneous transmission emission thallium-201 cardiac SPECT: effect of attenuation correction on myocardial tracer distribution. *J Nucl Med* 1995;36:921–931.
19. Bacharach SL, Buvat I. Attenuation correction in cardiac positron emission tomography and single-photon emission tomography. *J Nucl Cardiol* 1995;2:246–255.Q1: Au: Cite affilliation for Ziegler and Bonning in Acknowledgments in English.

Reproducibility of Measurements of Regional Resting and Hyperemic Myocardial Blood Flow Assessed with PET

Shigeki Nagamachi, Johannes Czernin, Anatole S. Kim, Karl T. Sun, Morten Böttcher, Michael E. Phelps and Heinrich R. Schelbert

Department of Molecular and Medical Pharmacology, Division of Nuclear Medicine, UCLA School of Medicine; and Laboratory of Structural Biology and Molecular Medicine, University of California, Los Angeles, California

PET with ^{13}N-ammonia permits the noninvasive quantification of myocardial blood flow (MBF) in humans. The present study was done to assess the reproducibility of quantitative blood flow measurements at rest and during pharmacologically induced hyperemia in healthy individuals. **Methods:** Thirty healthy volunteers (26 men, 4 women) were studied. Paired measurements of MBF at rest (n = 21), during adenosine (n = 15) and during dipyridamole (n = 7) were performed using a two-compartment model for ^{13}N-ammonia PET. The mean difference between baseline and follow-up blood flow (% difference) was calculated to assess reproducibility. **Results:** No significant difference was observed between resting blood flow at baseline or follow-up (15.8% ± 15.8%; p = ns). Baseline and follow-up resting blood flow were linearly correlated (r = 0.63, p < 0.005). Normalization of resting blood flow to the rate pressure product improved the reproducibility significantly (15.8% ± 15.8% versus 10.1% ± 10.5%, p < 0.05). Baseline and follow-up hyperemic myocardial blood flow did not differ (11.8% ± 9.4%; p = ns) and were linearly correlated (r = 0.69, p < 0.0005). **Conclusion:** MBF at rest can be measured reproducibly with ^{13}N-ammonia PET. The individual response to pharmacologic stress appears to be relatively consistent. Thus, serial blood flow measurements with ^{13}N-ammonia PET can be used to quantify the effect of various interventions on MBF and vasodilatory reserve.

Key Words: myocardial blood flow; pharmacologic stress; PET

J Nucl Med 1996; 37:1626–1631

PET with either ^{13}N-ammonia or ^{15}O-water and an appropriate tracer compartmental model allows for noninvasive quantification of myocardial blood flow (MBF) (*1–7*). Such measurements have been used in healthy volunteers (*1–3,8,9*), patients with coronary artery disease (*3,10,11*) and other cardiac diseases (*12,13*). Additionally, these measurements have been used to assess the effect of pharmacologic intervention (*14*), cardiovascular conditioning (*15*), coronary angioplasty (*16,17*) and immunosuppressive treatment on rejecting heart transplant on MBF (*18*).

The reproducibility of regional MBF measurements with ^{13}N-ammonia and dynamic PET, however, has yet to be extensively examined (*19*). Establishing the reproducibility of this method would be particularly important for serial PET measurements of MBF after pharmacologic or therapeutic interventions.

Thus, the aim of the current study was to determine the reproducibility of ^{13}N-ammonia PET measurements of MBF at rest and during pharmacologically induced hyperemia in a group of healthy individuals.

MATERIALS AND METHODS

Subjects

Thirty healthy volunteers (26 men, 4 women) with a mean age of 33.7 ± 15.4 yr and a low likelihood for coronary artery disease were included in this study (*20*). None of the participants were taking any medication and all refrained from caffeine intake 24 hr before the PET study (*21*). Each participant signed an informed consent form approved by the UCLA Human Subject Protection Committee.

Study Protocol

Paired resting MBF studies were performed in eight individuals within the same day. Also within the same day, nine other participants had paired hyperemic blood flow studies during intravenous adenosine. Lastly, both paired resting and paired hyperemic blood flow studies (adenosine; n = 6 or dipyridamole; n = 7) were obtained in the 13 remaining participants at an average time interval of 26.5 ± 18.9 days.

Adenosine and dipyridamole induce comparable degrees of myocardial hyperemia (*9*). The relatively long half-life of dipyridamole (30 min), however, precludes serial hyperemic blood flow studies within the same day (*22*). Adenosine has a short half-life of < 5 sec (*23*). Therefore, the reproducibility of hyperemic blood flow within the same day was tested with adenosine while the reproducibility of hyperemic blood flow measurements on separate occasions was assessed with dipyridamole.

Adenosine was infused intravenously at a rate of 140 μg/kg for 6 min. Three minutes after the start of the adenosine infusion, 370–555 MBq of ^{13}N-ammonia were injected intravenously over 30 sec while the serial PET image acquisition was started. For dipyridamole induced hyperemia, dipyridamole (0.56 mg/kg) was infused intravenously over 4 min (*24*). Four minutes later, 370–555 MBq of ^{13}N-ammonia was injected over 30 sec and the serial

Received Aug. 18, 1995; revision accepted Dec. 13, 1995.
For correspondence or reprints contact: Johannes Czernin, MD, Department of Molecular and Medical Pharmacology, B2-085 J CHS, 10833 Le Conte Avenue University of California, Los Angeles, CA 90024-6948.

imaging sequence commenced. For the one-day protocol, each study was separated by 50 min (>5 half-lives of ^{13}N) to allow for decay of radioactivity. Motion artifacts were minimized by fastening a Velcro strap across the volunteer's chest. ECG was monitored continuously. Heart rate and blood pressure (cuff measurements) were measured 1-min intervals during the first 2 min of tracer injection.

Image Acquisition

All studies were performed on a PET scanner that acquires 15 transaxial images simultaneously (*25*). The tomographic images were reconstructed using a Shepp filter with a cutoff of 0.3 Nyquist frequency, resulting in an effective in-plane resolution of 11 mm FWHM. To correct for photon attenuation, a 20-min transmission image was performed before each imaging sequence. The dynamic imaging sequences consisted of 12 frames: 10 sec each, 2 frames of 30 sec each, 1 frame of 60 sec and 1 frame of 90 sec.

Quantification of Myocardial Blood Flow

The 15 transaxial images were re-oriented into six short axis planes as described previously (*5*). Three, 70°-90° sectorial regions of interest (ROIs) were assigned to the anterior, lateral and inferior wall on a basilar, midventricular and more apical short-axis cross-section of the left ventricular myocardium (*8*). The three sectorial regions of interest correspond to the territories of the left anterior descending, the left circumflex and the right coronary artery.

To assign comparable ROIs between studies as well as between individuals, the insertion of the right ventricle into the intraventricular septum served as anatomical landmark and a starting point for the placement of the regions. The regions were then copied to the first 120 sec (12 frames) of the dynamic imaging sequence to obtain regional tissue time activity curves. The time activity curves were averaged between three planes to obtain one time activity curve for each vascular territory (LAD, LCX, RCA). In addition, the three regional time activity curves were averaged to obtain a single time activity curve for each individual (*8*). A 25-mm^2 ROI (10 pixels) was placed in the left ventricular blood pool and copied to the first 12 frames (120 sec) of the serial acquired images to obtain the arterial input function (*26*).

Regional and averaged tissue time-activity curves were corrected for partial volume effects by assuming a uniform wall thickness of 1 cm (*27*). They were also corrected for spillover of activity from the blood pool to the myocardium and for physical decay of the ^{13}N (*26*). The corrected blood-pool and myocardial time-activity curves were fitted with a previously validated two-compartment tracer kinetic model (*4,6*).

Statistical Analysis

The reproducibility of the measurements was assessed by linear regression analysis and the difference between the baseline and follow-up measurements. The percent difference was calculated as follows: follow-up blood flow−baseline blood flow/baseline blood flow × 100. Mean values are given with their s.d. The paired t-test was used to compare hemodynamic parameters and MBF within each participant. Analysis of variance was used to evaluate differences between groups and interventions of protocols. Correlations were sought using least squares regression analysis. Probability (p) values < 0.05 were considered statistically significant.

RESULTS

Semiquantitative Polar Map Activity Analysis

The short-axis images were assembled into polar maps of the ^{13}N-ammonia activity distribution and compared with a database of normal volunteers (*28*). All participants had a homogeneous tracer distribution throughout the entire left ventricular myocardium at baseline and follow-up by polar map analysis, suggesting that the participants were indeed free of significant coronary artery disease (*29–31*).

TABLE 1
Hemodynamic Findings

	Baseline	Follow-up	Differences (%)
Rest (n = 21)			
Heart rate (bpm)	62 ± 11	66 ± 13	9.2 ± 10.0
SBP (mmHg)	115 ± 12	112 ± 10	4.8 ± 4.6
DBP (mmHg)	68 ± 12	67 ± 11	7.9 ± 7.4
RPP (bpm · mmHg)	7151 ± 1518	7360 ± 1737	16.5 ± 11.5
MABP (mmHg)	84 ± 11	82 ± 10	4.7 ± 3.3
Stress (n = 22)			
Heart rate (bpm)	93 ± 12	95 ± 14	8.3 ± 7.4
SBP (mmHg)	119 ± 11	116 ± 11	5.1 ± 5.0
DBP (mm Hg)	67 ± 10	65 ± 8	6.8 ± 4.8
RPP (bpm · mmHg)	11083 ± 2068	10958 ± 2185	8.8 ± 7.2
MABP (mmHg)	84 ± 9	81 ± 8	5.5 ± 4.5
(Adenosine; n = 15)			
Heart rate (bpm)	95 ± 12	95 ± 15	6.9 ± 5.5
SBP (mmHg)	121 ± 12	118 ± 12	4.5 ± 4.9
DBP (mmHg)	66 ± 12	65 ± 10	7.7 ± 5.4
RPP (bpm · mmHg)	11459 ± 2205	11254 ± 2318	7.7 ± 6.5
MABP (mmHg)	84 ± 10	82 ± 9	5.9 ± 4.8
(Dipyridamole; n = 7)			
Heart rate (bpm)	88 ± 11	93 ± 13	7.0 ± 14.0
SBP (mmHg)	116 ± 9	111 ± 8	6.3 ± 5.3
DBP (mmHg)	66 ± 6	67 ± 6	5.1 ± 2.6
RPP (bpm · mmHg)	10277 ± 1587	10324 ± 1868	11.1 ± 8.7
MBP (mmHg)	84 ± 7	81 ± 6	4.8 ± 4.1

SBP = systolic blood pressure; DBP = diastolic blood pressure; MABP; mean aortic blood pressure; RPP = rate pressure product (heart rate × SBP)

Hemodynamic Findings

Resting systolic blood pressure, diastolic blood pressure, mean aortic blood pressure, heart rate and rate pressure product did not differ significantly between the two studies (Table 1). Similarly, systolic, diastolic and mean aortic blood pressure as well as heart rate and rate pressure product were comparable during the paired hyperemic blood flow studies (Table 1).

Myocardial Blood Flow at Rest

Resting blood flow averaged 0.62 ± 0.14 at baseline and 0.66 ± 0.15 ml/g/min at follow up (p = ns; Table 2). Mean

TABLE 2
Myocardial Blood Flow at Rest (n = 21)

	Baseline	Follow-up	Differences (%)
Resting blood flow (ml/g/min)			
Mean	0.62 ± 0.14	0.66 ± 0.15	15.8 ± 15.8
LAD	0.59 ± 0.13	0.63 ± 0.14	12.5 ± 13.2
LCX	0.65 ± 0.21	0.66 ± 0.19	21.1 ± 23.5
RCA	0.64 ± 0.14	0.68 ± 0.14	19.0 ± 16.2
Normalized resting blood flow (ml/g/min/RPP)			
Mean	0.08 ± 0.01	0.09 ± 0.02	10.1 ± 10.5*
LAD	0.08 ± 0.01	0.09 ± 0.01	9.9 ± 9.6
LCX	0.09 ± 0.01	0.09 ± 0.02	16.8 ± 15.8
RCA	0.09 ± 0.01	0.09 ± 0.02	14.5 ± 12.0

*$p < 0.05$ vs. % differences of mean absolute blood flow (%).
LAD = left anterior descending coronary artery; LCX = left circumflex coronary artery; RCA = right coronary artery; RPP = rate pressure product.

TABLE 3
Comparison of Percent Differences between One-day and Two-day Protocols

	One-day	Two-day	
Rest	(n = 8)	(n = 13)	
Mean resting blood flow (%)	12.0 ± 10.1	18.1 ± 17.7	ns
Mean normalized resting blood flow (%)	7.7 ± 6.9	11.5 ± 12.2*	
Stress	(n = 9)	(n = 13)	
Mean hyperemic blood flow (%)	12.2 ± 8.1	11.4 ± 11.5	ns
Mean coronary vascular resistance index (%)	11.6 ± 10.2	10.3 ± 10.5	ns

*$p < 0.05$
ns = nonsignificant

blood flow within each individual differed by 15.8% ± 15.8% between the studies. Resting blood flow was correlated with the rate pressure product at baseline ($r = 0.88$, $p < 0.0001$) and at follow-up ($r = 0.74$, $p < 0.0001$).

Regional resting blood flow was similar in the three vascular territories both at baseline and at follow-up. The relative differences in regional resting blood flow are listed in Table 2. Interstudy differences in regional MBF ranged from 0.00 to 0.28, 0.00 to 0.54 and 0.01 to 0.35 ml/g/min and averaged 0.07 ± 0.07, 0.14 ± 0.14 and 0.11 ± 0.09 ml/g/min in the left anterior descending, left circumflex and right coronary artery territories, respectively.

To account for individual differences in cardiac work (*8*), resting blood flow was normalized to the rate pressure product (RPP). Mean normalized MBF did not differ significantly between the baseline and the follow-up study and differed by 10.1% ± 10.5% (Table 2). The percent difference of mean normalized MBF was significantly smaller than that of absolute myocardial blood flow ($p < 0.05$).

The percent difference in resting blood flow tended to be larger for the two day than for the one day protocol. No significant differences, however, were observed (Table 3).

TABLE 4
Hyperemic Blood Flow

	Baseline	Follow-up	Differences (%)
MBF (n = 22)			
Mean	2.01 ± 0.39	2.03 ± 0.31	11.8 ± 9.4
LAD	1.93 ± 0.39	1.94 ± 0.32	11.9 ± 9.1
LCX	1.95 ± 0.43	2.02 ± 0.36	13.5 ± 12.1
RCA	2.14 ± 0.43	2.14 ± 0.36	15.2 ± 12.1
CVR (n = 22)			
Mean	43.34 ± 9.05	41.28 ± 7.80	10.8 ± 10.1
LAD	45.18 ± 9.73	45.45 ± 8.79	11.7 ± 9.2
LCX	45.08 ± 10.76	41.87 ± 9.07	10.8 ± 10.2
RCA	40.75 ± 8.50	39.46 ± 8.16	13.9 ± 14.8
Adenosine (n = 15)			
Mean MBF	1.97 ± 0.45	2.05 ± 0.33	12.2 ± 10.3
Mean CVR	44.64 ± 0.45	41.25 ± 8.42	10.4 ± 9.7
Dipyridamole (n = 7)			
Mean MBF	2.09 ± 0.25	2.00 ± 0.31	10.8 ± 7.5
Mean CVR	40.57 ± 6.73	41.33 ± 6.89	11.7 ± 11.8

MBF = myocardial blood flow (ml/g/min); CVR = coronary vascular resistance index (mmHg/ml/g/min); LAD = left anterior descending artery; LCX = left circumflex coronary artery; RCA = right coronary artery.

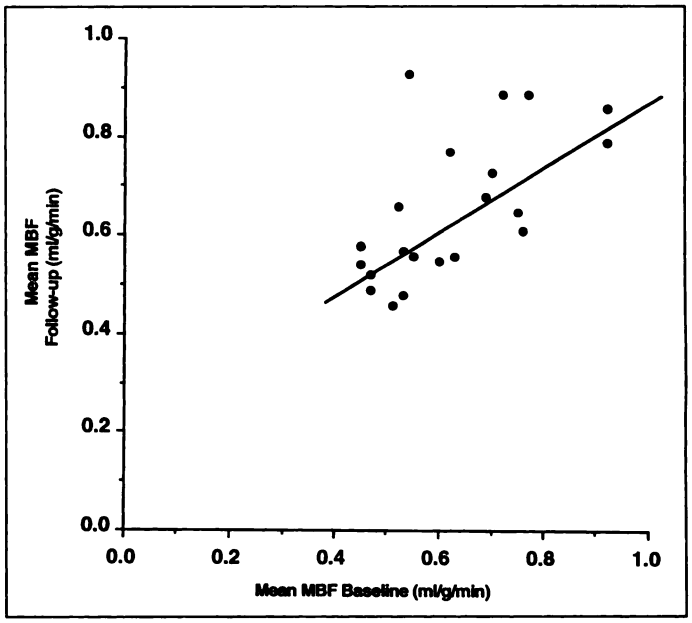

FIGURE 1. Scatter plot of the relationship between baseline and follow-up study of resting MBF (n = 21). Initial and repeat measurements of perfusion were correlated by $y = 0.65x + 0.25$, $r = 0.63$, $p < 0.005$; s.e.e.:0.12.

Moreover, the reproducibility of blood flow measurements on different days was improved by normalizing blood flow to the rate pressure product (18.1 ± 17.7 versus 11.5% ± 12.2%; $p < 0.05$).

Hyperemic Myocardial Blood Flow

Pharmacologic vasodilation was induced by adenosine in 15 patients and by dipyridamole in 7. Both substances induced a similar degree of myocardial hyperemia (Table 4). Mean hyperemic blood flow differed by 11.8% ± 9.4% (p=ns). The absolute differences ranged from 0.02 to 0.68 ml/g/min and averaged 0.22 ± 0.17 ml/g/min.

Regional hyperemic blood flow did not differ between the three territories or between baseline and follow-up study (Table 4). The percent differences between baseline and follow-up study are summarized in Table 4. The individual differences in hyperemic blood flow ranged from 0.00 to 0.63, 0.00 to 0.58 and 0.05 to 0.87 ml/g/min and averaged 0.23 ± 0.17, 0.25 ± 0.19 and 0.31 ± 0.23 ml/g/min in the territories of the LAD, LCX and RCA, respectively (Table 4).

An index of coronary vascular resistance (CVR) was estimated from the ratio of mean aortic blood pressure to blood flow (*32*). This resistance index did not differ between baseline or follow-up. Similarly, it did not differ between the three vascular territories or between baseline and follow up (Table 4). The changes in resistance index were similar to those observed for absolute regional MBF. No significant differences in hyperemic blood flow or resistance index were noted between the one-day and two-day protocols (Table 3).

Overall Reproducibility of Blood Flow Measurements

Overall, all mean baseline and all follow-up blood flow measurements were closely correlated with a slope approaching unity ($y = 0.93x + 0.12$, $r = 0.96$; $p < 0.0001$). There was a significant correlation between baseline and follow-up MBF at rest ($r = 0.63$, $p < 0.005$; Fig. 1). The regional blood flow measurements were also significantly correlated ($r = 0.73$, $p < 0.0001$ in the LAD, $r = 0.51$, $p < 0.05$ in the LCX and $r = 0.49$, $p < 0.05$ in the RCA). Similarly, a significant correlation was found between baseline and follow-up for mean normalized resting blood flow ($r = 0.60$, $p < 0.005$; Fig. 2). The y-intercept

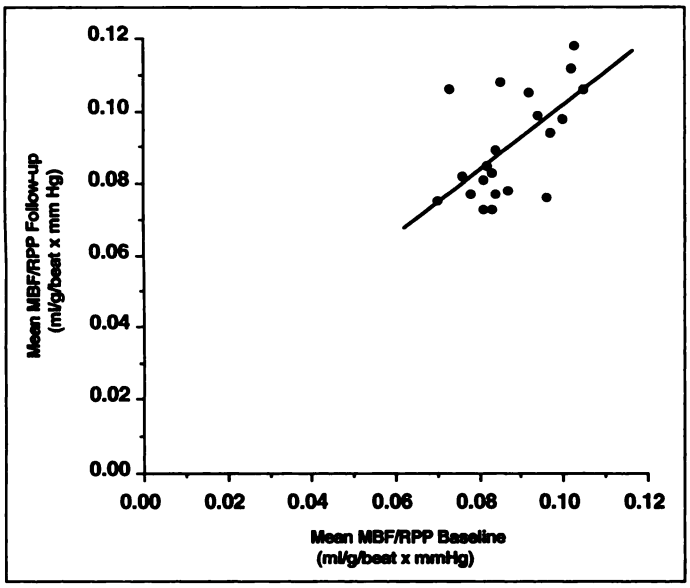

FIGURE 2. Scatter plot of the relationship between baseline and follow-up resting MBF normalized to the rate pressure product (n = 21). Baseline data correlated linearly with the follow-up data by y = 0.86x + 0.015, r = 0.60, p < 0.005; s.e.e.:0.012.

was positive likely due to the narrow range of resting blood flow values (Fig. 1). Note, that the slope was markedly improved when blood flow was normalized to the rate pressure product (Fig. 2).

Measurements of hyperemic blood flow, induced by dipyridamole, were as reproducible as those induced by adenosine (Table 4). Overall, mean (r = 0.69, p < 0.0005, Fig. 3) and regional hyperemic baseline and follow-up blood flow also significantly correlated (r = 0.70, p < 0.0005 in the LAD, r = 0.71, p < 0.0001 in the LCX and r = 0.53, p < 0.01 in the RCA). Again, small ranges of hyperemic blood flow values likely explain the positive y-intercept of the relationship (Fig. 3).

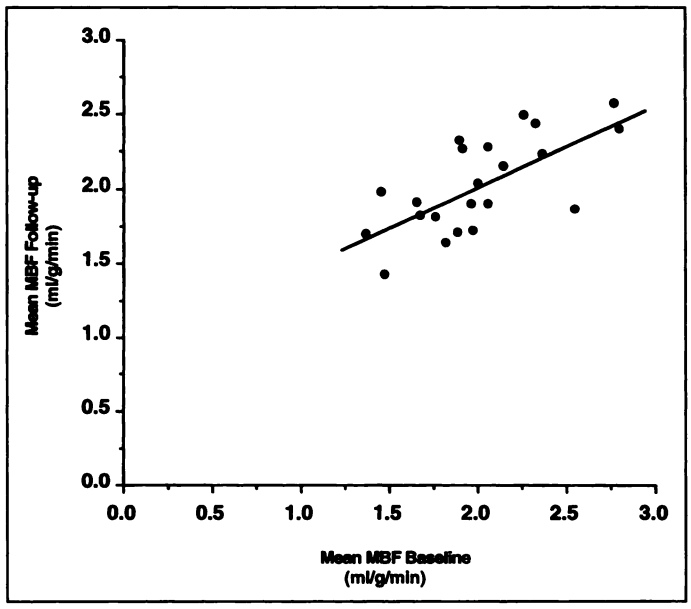

FIGURE 3. Scatter plot of the relationship between baseline and follow-up hyperemic MBF (n = 22). Baseline and follow-up measurements of perfusion were correlated by y = 0.55x + 0.93, r = 0.69, p < 0.0005; s.e.e.: 0.23.

DISCUSSION

MBF at rest and during pharmacologically induced hyperemia can be measured reproducibly with ^{13}N-ammonia and PET in the same study session as well as on different days.

Several methodological problems such as: the participant's motion, size and placement of myocardial tissue and blood-pool ROIs, and differences in spillover activity fraction between blood pool and myocardium might affect the reproducibility of quantitative blood flow measurements with PET.

Subject motion was minimized by fastening a Velcro strap across their chest. In addition, only the first 120 sec of activity data were used for quantitative analysis. Thus, motion is unlikely to have contributed significantly to the observed variability.

Kuhle et al. (*6*) reported a 2.5 times greater s.e.e. for blood flow measurements derived from small ROIs (45° myocardial sectors) than for the averaged value of 20–24 sectors (*6*). Therefore, we used rather large, 70–90° ROI to assess blood flow in the E3 major vascular territories. This approach yields blood flow measurements with a relatively small coefficient of variation of less than 15% (*8*).

Spillover activity from blood pool to myocardial tissue was corrected by a deconvolution technique validated previously (*33*), but because of prominent biventricular spillover, the interventricular septum was excluded from quantitative analysis.

Reproducibility of Blood Flow at Rest

MBF at rest depends largely on cardiac work (*4,8,10,34,35*). Therefore, MBF at rest would be expected to vary with the rate-pressure product, the most commonly used index of cardiac work. Because this index of cardiac work varied by about 16% (Table 1), MBF at rest varied to a similar degree between the studies (Table 2). The rate pressure product varied considerably between individuals, which explains, in part, the variability of resting blood flow which ranged from 0.45 to 0.93 ml/g/min in the current study. Consequently, myocardial blood flow normalized to the rate pressure product reduced the variability of measurements significantly from 15.8% ± 15.8% to 10.1% ± 10.5%. Thus, to allow meaningful interpretation of quantitative data, resting blood flow should be normalized to the rate pressure product.

Reproducibility of Hyperemic Blood Flow

The reproducibility of PET derived blood flow measurements during pharmacologically induced hyperemia depends upon several methodological and physiological parameters. Among these are: (a) variation in time interval from the infusion of the pharmacologic stress agent to administration of the blood flow tracer (*22*), (b) changes in physiologic determinants of blood (*22,36*) flow such as heart rate (*37*) or (c) coronary driving pressure (*38,39*).

The response to dipyridamole changes over time with a relatively constant and maximal response occurring 8 min after the beginning of the vasodilator infusion (*21*). Accordingly, ^{13}N-ammonia was injected consistently at that time. A similarly rigorous schedule was used for the hyperemic study during intravenous adenosine with tracer injection 3 min after start of adenosine (*24,35,37*). Therefore, differences in the study protocol were unlikely to have contributed to the observed variability in blood flow.

Animal experimental studies have suggested that increases in heart rate might reduce hyperemic blood flow by shortening the diastolic flow phase (*37*). McGinn et al. (*40*) failed to observe an effect of tachycardia up to 120 bpm on hyperemic blood flow. Changes in heart rate were small between baseline and

follow-up. Therefore, they were unlikely to have affected the reproducibility of hyperemic blood flow.

Coronary driving pressure (*41*), another important determinant of hyperemic blood flow, was relatively stable between the two hyperemic studies. This might partly explain the small changes in hyperemic blood flow between studies. To examine whether the small changes in mean arterial blood pressure contribute to the observed variability, an index of coronary vascular resistance was derived from the ratio of mean aortic blood pressure to myocardial blood flow (*32,38,39,41*). Such correction did not improve the reproducibility of hyperemic blood flow measurements.

Considerable variability of hyperemic blood flow was observed in the territory of the right coronary artery. Again, biventricular spillover from the inferior aspect of the intraventricular septum as well as activity spillover from the liver to the inferior wall of the left ventricle might have compromised the time-activity curves in some subjects and might explain this variability.

Study Limitations

One limitation of this investigation is that only healthy individuals were studied. Thus, the reproducibility of blood flow measurements derived from smaller ROIs patients with coronary artery disease remains unknown.

Another limitation of the study is a uniform left ventricular wall thickness of 1 cm was assumed in each participant for partial volume correction. In patients with left ventricular hypertrophy or coronary artery disease, different recovery coefficients derived from echocardiographic wall thickness measurements need to be employed for correction of partial volume effects.

CONCLUSION

The current study demonstrated a significant reproducibility of noninvasively derived quantitative MBF measurements with ^{13}N-ammonia PET, suggesting that they can be used for noninvasively monitoring the effect of revascularization procedures, pharmacological interventions or risk factor modifications on MBF and flow reserve. The considerable variability in regional MBF observed in the current study, however, suggests that such serial measurements need to be interpreted with caution.

ACKNOWLEDGMENTS

We thank Ron Sumida, Larry Pang, Francine Aguilar, Marc Hulgan and Derjenn Liu for their technical assistance. This study was operated for the U.S. Department of Energy by the University of California under Contract #DE-FC03-87ER60615. This work was supported in part by the Director of the Office of Energy Research, Office of Health and Environmental Research, Washington, D.C. (research grants #HL 29845 and #HL 33177), National Institutes of Health, Bethesda, MD and by an Investigative Group Award by the Greater Los Angeles Affiliate of the American Heart Association, Los Angeles, CA.

REFERENCES

1. Bergmann SR, Fox KAA, Rand AL, et al. Quantification of regional myocardial blood flow in vivo with H2^{15}O. *Circulation* 1984;70:724–733.
2. Hutchins G, Schwaiger M, Rosenspire K, Krivokapich J, Schelbert H, Kuhl D. Noninvasive quantification of regional blood flow in the human heart using ^{13}N ammonia and dynamic positron emission tomographic imaging. *J Am Coll Cardiol* 1990;15:1032–1042.
3. Iida H, Kanno I, Takahashi A, Miura S, et al. Measurement of absolute myocardial blood flow with H2^{15}O and dynamic positron emission tomography. Strategy for quantification in relation to the partial-volume effect. *Circulation* 1988;78:104–115.
4. Krivokapich J, Smith GT, Huang SC, et al. Nitrogen-13-ammonia myocardial imaging at rest and with exercise in normal volunteers. Quantification of absolute myocardial perfusion with dynamic positron emission tomography. *Circulation* 1989;80:1328–1337.
5. Kuhle W, Porenta G, Huang SC, Phelps M, Schelbert H. Issues in the quantitation of re-oriented cardiac PET images. *J Nucl Med* 1992;33:1235–1242.
6. Kuhle W, Porenta G, Huang SC, et al. Quantification of regional myocardial blood flow using ^{13}N-ammonia and re-oriented dynamic positron emission tomographic imaging. *Circulation* 1992;86:1004–1017.
7. Schelbert HR, Phelps ME, Huang SC, et al. Nitrogen-13- ammonia as an indicator of myocardial blood flow. *Circulation* 1981;63:1259–1272.
8. Czernin J, Müller P, Chan S, et al. Influence of age and hemodynamics on myocardial blood flow and flow reserve. *Circulation* 1993;88:62–69.
9. Chan S, Brunken R, Czernin J, et al. Comparison of maximal myocardial blood flow during adenosine infusion with that of intravenous dipyridamole in normal men. *J Am Coll Cardiol* 1992;20:979–985.
10. Czernin J, Porenta G, Brunken R, et al. Regional blood flow, oxidative metabolism and glucose utilization in patients with recent myocardial infarction. *Circulation* 1993;88:884–895.
11. Sambuceti G, Parodi O, Marcassa C, et al. Alteration in regulation of myocardial blood flow in one-vessel coronary artery disease determined by positron emission tomography. *Am J Cardiol* 1993;72:538–543.
12. Camici P, Chiriatti G, Oorenzoni R, et al. Coronary vasodilation is impaired in both hypertrophied and nonhypertrophied myocardium of patients with hypertrophic cardiomyopathy: a study with nitrogen-13-ammonia and positron emission tomography. *J Am Coll Cardiol* 1991;17:879–886.
13. Nienaber C, Gambhir S, Vaghaiwalla Mody F, et al. Regional myocardial blood flow and glucose utilization in symptomatic patients with hypertrophic cardiomyopathy. *Circulation* 1993;87:1580–1590.
14. Bottcher M, Czernin J, Phelps M, Schelbert H. Beneficial effect of β-blockade on myocardial blood flow and vasodilator capacity in humans [Abstract]. *J Am Coll Cardiol* 1995;22:427A.
15. Czernin J, Barnard RJ, Sun KT, et al. Beneficial effect of cardiovascular conditioning on myocardial blood flow and coronary vasodilator capacity. *Circulation* 1995;92:197–204.
16. Uren NG, Crake T, Lefroy DC, DeSilva R, Davies GJ, Maseri A. Delayed recovery of coronary resistive vessel function after coronary angioplasty. *J Am Coll Cardiol* 1993;21:612–621.
17. Walsh MN, Geltman EM, Steele RL, et al. Augmented myocardial perfusion reserve after coronary angioplasty quantified by positron emission tomography with H2^{15}O. *J Am Coll Cardiol* 1990;15:119–127.
18. Chan SY, Kobashigawa J, Stevenson LW, Brownfield E, Brunken RC, Schelbert HR. Myocardial blood flow at rest and during pharamacological vasodilation in cardiac transplants during and after successful treatment of rejection. *Circulation* 1994;90:204–212.
19. Sawada S, Muzik O, Beanlands R, Wolfe E, Hutchins G, Schwaiger M. Interobserver and interstudy variability of myocardial blood flow and flow-reserve measurements with nitrogen-13-ammonia labeled positron emission tomography. *J Nucl Cardiol* 1995;2:413–422.
20. Diamond G, Forrester J. Analysis of probability as an aid in the clinical diagnosis of coronary artery disease. *N Engl J Med* 1979;300:1350–1358.
21. Smits P, Thien TH, van't Laar A. Circulatory effects of coffee in relation to the pharmacokinetics of caffeine. *Am J Cardiol* 1985;56:958–963.
22. Brown BG, Josephson MA, Peterson RB, et al. Intravenous dipyridamole combined with isometric handgrip for near maximal acute increase in coronary flow in patients with coronary artery disease. *Am J Cardiol* 1981;48:1077–1085.
23. Olsson RA, Pearson JD. Cardiovascular purinoceptors. *Physiol Rev* 1990;70:761–84.
24. Wilson R, Laughlin D, Ackell P, et al. Transluminal subselective measurement of coronary blood flow velocity and vasodilator reserve in man. *Circulation* 1985;72:82–92.
25. Spinks TJ, Guzzardi R, Bellina CR. Performance characteristics of a whole-body positron tomograph. *J Nucl Med* 1988;29:1833–1841.
26. Weinberg IN, Huang SC, Hoffman EJ, et al. Validation of PET-acquired functions for cardiac studies. *J Nucl Med* 1988;29:241–247.
27. Gambhir SS, Schwaiger M, Huang SC, et al. Simple noninvasive quantification method for measuring myocardial glucose utilization in humans employing positron emission tomography and fluorine-18-deoxyglucose. *J Nucl Med* 1989;30:359–366.
28. Porenta G, Kuhle W, Czernin J, et al. Semiquantitative assessment of myocardial viability and perfusion utilizing polar map displays of cardiac PET images. *J Nucl Med* 1992;33:1623–1631.
29. Demer LL, Gould KL, Goldstein RA, et al. Assessment of coronary artery disease severity by positron emission tomography. Comparison with quantitative arteriography in 193 patients. *Circulation* 1989;79:825–835.
30. Schelbert HR, Wisenberg G, Phelps ME, Gould KL, et al. Noninvasive assessment of coronary stenoses by myocardial imaging during pharmacologic coronary vasodilation. VI. Detection of coronary artery disease in man with intravenous ^{13}N ammonia and positron computed tomography. *Am J Cardiol* 1982;49:1197–1207.
31. Tamaki N, Yonekura Y, Senda M, et al. Value and limitation of stress thallium-201 single-photon emission computed tomography: comparison with nitrogen-13-ammonia positron tomography. *J Nucl Med* 1988;29:1181–1188.
32. Marcus M. Autoregulation in the coronary circulation. In: Marcus M, ed. *The coronary circulation in health and disease*. New York: McGraw-Hill;1983:93–112.
33. Henze E, Huang SC, Ratib O, Hoffman E, Phelps ME, Schelbert HR. Measurement of regional tissue and blood-pool radiotracer concentrations from serial tomographic images of the heart. *J Nucl Med* 1983;24:987–996.
34. Müller P, Czernin J, Choi Y, et al. Effect of exercise supplementation during adenosine infusion on hyperemic blood flow and flow reserve. *Am Heart J* 1994;128:52–60.
35. Klocke F, Mates R, Canty JJ, Ellis A. Coronary pressure-flow relationship. Controversial issues and probable implications. *Circ Res* 1985;56:310–323.
36. Rossen J, Quillen J, Lopez A, Stenberg R, Talman C, Winniford M. Comparison of coronary vasodilation with intravenous dipyridamole and adenosine. *J Am Coll Cardiol* 1991;18:485–491.

37. Bache R, Cobb F. Effect of maximal coronary vasodilation on transmural myocardial perfusion during tachycardia in the awake dog. *Circ Res* 1977;41:648–653.
38. Hoffman E. Maximal coronary flow and the concept of coronary vascular reserve. *Circulation* 1984;70:153–165.
39. Ohtsuka S, Kakihana M, Sugishita Y, Ito I. Effects of the rise in aortic blood pressure on coronary flow reserve in dogs. *Jpn Heart J* 1987;28:403–412.
40. McGinn A, White C, Wilson R. Interstudy variability of coronary flow reserve: Influence of heart rate, arterial pressure and ventricular preload. *Circulation* 1990;81: 1319–1330.
41. Klocke F, Ellis A, Canty J, Jr. Interpretation of changes in coronary flow that accompany pharmacologic interventions. *Circulation* 1987;75(suppl V):34–38.

Comparison of Myocardial Uptake of Fluorine-18-Fluorodeoxyglucose Imaged with PET and SPECT in Dyssynergic Myocardium

Jeroen J. Bax, Frans C. Visser, Paul K. Blanksma, Magreet A. Veening, Eng S. Tan, Antoon T.M. Willemsen, Arthur van Lingen, Gerrit J.J. Teule, Willem Vaalburg, Kong I. Lie and Cees A. Visser
Departments of Cardiology and Nuclear Medicine, Free University Hospital Amsterdam; and the PET Center of the Groningen University Hospital, Groningen, The Netherlands

PET with ^{18}F-fluorodeoxyglucose (FDG) can detect viable myocardium and predict functional recovery after revascularization. The use of PET for clinical routine, however, is limited. Recently, imaging FDG with SPECT was proposed. The aim of this study was to compare the diagnostic value of FDG-PET and FDG-SPECT in the detection of viable myocardium in segments with abnormal wall motion. **Methods:** Twenty patients with previous myocardial infarction were studied. All underwent FDG-PET and FDG-SPECT during hyperinsulinemic glucose clamping. Regional perfusion was assessed with ^{13}N-ammonia PET and early resting ^{201}Tl- SPECT. Regional wall motion was assessed with two-dimensional echocardiography. The agreement between FDG/^{13}N-ammonia PET and FDG/^{201}Tl SPECT to detect viability in dyssynergic myocardium was 76%. On a patient basis, PET and SPECT yielded comparable results in 17 of 20 patients. In a subgroup of patients with LVEF ≤ 35% (n = 12), all PET and SPECT viability data were identical. **Conclusion:** This study shows a good correlation between the detection of viability in dyssynergic myocardium with FDG/^{13}N-ammonia PET and FDG/^{201}Tl SPECT, both on a segmental and patient basis.

Key Words: PET; fluorine-18-fluorodeoxyglucose; SPECT; myocardial viability

J Nucl Med 1996; 37:1631–1636

Dyssynergic but viable myocardium can be detected with PET using ^{18}F-fluorodeoxyglucose (FDG) (*1–4*). PET centers, however, are not widely available to meet the clinical demand for viability studies with FDG. Several institutions have recently studied the feasibility of imaging myocardial FDG uptake with SPECT (*5–10*). Two recent reports described good agreement between myocardial FDG uptake assessed with PET and SPECT (*8,10*). Moreover, we have previously shown that FDG-SPECT can predict improvement of regional contractile function after revascularization (*11*).

In this study, we compared the diagnostic value of FDG-PET and FDG-SPECT in the detection of residual viability in dyssynergic myocardium (assessed by echocardiography). For comparison, not only was FDG uptake considered, but also its uptake relative to a flow tracer (^{13}N-ammonia in the PET study and ^{201}Tl in the SPECT study). Quantitative analysis techniques were applied to the PET and SPECT data, to minimize observer bias.

Received Sept. 27, 1995; revision accepted Jan. 24, 1996.
For correspondence or reprints contact: Jeroen J. Bax, MD, Department of Cardiology, University Hospital Leiden, Rijnsburgerweg 10, 2333 AA Leiden, The Netherlands.

MATERIALS AND METHODS

Patients and Study Protocol

Twenty patients (4 women, 16 men; mean age 64 ± 8 yr) with previous infarction were included. Six patients had a non-Q wave infarction, and 14 had a Q wave on the ECG (6 inferior, 7 anterior and 1 both anterior and inferior). The mean time interval of infarction to the study was 42 ± 57 mo. All patients who underwent catheterization, had significant coronary artery disease on angiography (>50% reduction in luminal diameter of at least one major epicardial coronary artery (*25*)). Ten had three-vessel disease, five had two-vessel disease and three had single-vessel disease. They had a mean left ventricular ejection fraction (LVEF) of 39% ± 16% (12 patients had LVEF ≤ 35%). Four patients had diabetes mellitus type II and were well regulated on oral hypoglycemics. All patients underwent PET and SPECT studies to evaluate myocardial viability in dyssynergic myocardium. The mean time interval between the PET and SPECT studies was 34 ± 20 days (range 6–62 days). The investigators analyzing the PET, SPECT or echocardiographic data were unaware of the results of the other modalities. Cardiac catheterization was performed in 18 patients within 3 mo of the scintigraphic studies.

None of the patients experienced unstable angina pectoris or myocardial infarction during the study period. Cardiac medication remained unchanged during the entire study period. All patients gave informed consent to the study protocol that was approved by the Ethical Committee of the Free University Hospital Amsterdam.

Two-Dimensional Echocardiography

Echocardiography was performed within 2 wk of the scintigraphic studies. Four standard views of the left ventricle were obtained: parasternal long- and short-axis views and apical two- and four-chamber views. The images were reviewed off-line and consensus was achieved by two observers unaware of the PET/SPECT data. For comparison with the PET/SPECT data (Fig. 1) the left ventricle was divided into 13 segments (*12*). Both wall motion and thickening were analyzed. Each segment was assigned a wall motion score (WMS) of 0 to 3: normal = 0, hypokinetic = 1, akinetic = 2 and dyskinetic = 3.